IJRAME

INTERNATIONAL JOURNAL OF RESEARCH IN AERONAUTICAL AND MECHANICAL ENGINEERING
WWW.IJRAME.COM
ISSN (ONLINE): 2321-3051

Vol.12 Issue 9, September 2024
Pg:- 15 - 28

Shape Optimization in Low-Observable Aerodynamic Design

Sai Siddharth S[*] Praveen V[†] Srethan V P[‡] Sriram Paranthaman

Author Correspondence: siddharthaerospace@gmail.com, praveen2004.vp@gmail.com, srethanvp2003@gmail.com, sriramp@student.tce.edu

[*]***Sai Siddharth S, Dept of Mech, Thiagarajar College of Engineering.***

[†]***Praveen V, Dept of Mech, Thiagarajar College of Engineering.***

[‡]***Srethan V P , Dept of Mech, Thiagarajar College of Engineering.***

[§]***Sriram P, Dept of Mech, Thiagarajar College of Engineering.***

Abstract

This research explores the development of airfoils optimized for low-observable aerodynamic applications, balancing stealth characteristics with aerodynamic performance. A comprehensive analysis of over 100 NACA airfoils identified NACA 2412 and NACA 0012 as the optimal choice due to its favorable radar cross-section (RCS) and high lift-to-drag ratio (L/D), essential for subsonic efficiency. Initial aero- dynamic evaluations using XFLR5 supported the NACA 0012 2412's performance, aligning with previous findings (Li et al., 2016; Ander- son, 2011). Detailed CFD simulations with ANSYS Fluent, applying Reynolds-averaged Navier-Stokes (RANS) equations and the k-epsilon turbulence model, established a robust baseline for the airfoil's flow characteristics (Shyy et al., 2013; Versteeg and Malalasekera, 2007). To further refine the design, adjoint-based shape optimization was conducted using SU2, an open-source tool known for its advanced adjoint solvers and computational efficiency. Comparative analysis between the baseline ANSYS Fluent results and SU2-optimized simulations demonstrated significant performance improvements, including reduced drag and maintained lift and stability. This comparative study underscores SU2's effectiveness in enhancing stealth airfoil de- sign, reflecting its superior capability in high-fidelity aerodynamic optimization (Alonso et al., 2016-2024). The integration of SU2 into the design process highlights its potential for advancing low-observable aircraft technology.

Keywords: Fluid dynamics, Stealth design, Defence, Shape Optimization, SU2

IJRAME

INTERNATIONAL JOURNAL OF RESEARCH IN AERONAUTICAL AND MECHANICAL ENGINEERING
WWW.IJRAME.COM
ISSN (ONLINE): 2321-3051

Vol.12 Issue 9, September 2024
Pg:- 15 - 28

Introduction

The development of airfoils for low-observable aerodynamic applications re- quires a balance between stealth characteristics, such as a low radar cross- section (RCS), and effective aerodynamic performance in subsonic and low- supersonic regimes. In this research, a range of NACA airfoils, known for their aerodynamic versatility, were examined to find a suitable candidate. Key selection criteria focused on minimizing RCS while maintaining a high lift-to-drag ratio (L/D), which is critical for subsonic aircraft efficiency. From over 100 NACA airfoils, NACA 2412 and NACA 0012 emerged as the optimal choice due to its aerodynamic efficiency and favorable RCS characteristics, aligning with past research on airfoil selection for stealth applications (Li et al., 2016; Anderson, 2011) . Initial analyses of the selected airfoils were performed using XFLR5, a tool that combines lifting line theory and panel methods for airfoil and wing analysis. This software allowed for rapid parallel computation of aerodynamic characteristics such as L/D ratio, pitching moment, and drag across various angles of attack (AoA). The detailed performance evaluation, validated by research from Drela (1996) on low Reynolds number airfoil analysis, confirmed that NACA 2412 provided an excellent balance of aerodynamic performance and stealth requirements. These results were consistent with modern computational techniques for early-stage design, as highlighted by recent advancements in aerodynamic optimization published in the by Alonso and Jameson, 2005. To further refine our understanding of the NACA airfoil's performance, we conducted detailed CFD simulations using ANSYS Fluent.

These simulations were designed to explore critical factors such as pressure distribution, velocity profiles, and turbulence behavior around the airfoil under a range of flow conditions. The analysis utilized the Reynolds-averaged Navier-Stokes (RANS) equations in combination with the k-epsilon turbulence model, which provided a robust framework for accurately capturing the complex flow characteristics.

This approach aligns with contemporary CFD practices, as highlighted in the works of Shyy et al. (2013) and Versteeg and Malalasekera (2007), particularly in the context of turbulence modeling in aerodynamics. These initial simulations will serve as the baseline CFD analysis for this research. After we conduct adjoint based shape optimization, we will compare the optimized airfoil's performance against these baseline results. The optimization process, coupled with this baseline data, will demonstrate the airfoil's potential for future low-observable aircraft applications. As we move forward, we plan to leverage SU2 for CFD in the optimization phase. These open-source tools not only offer flexibility and advanced adjoint solvers but also improve computational efficiency, allowing us to further explore and refine the design. The comparison between the ANSYS Fluent baseline and the results from SU2 and Python solvers will highlight the potential gains in both performance and computational resource

utilization, offering valuable insights for future aircraft designs. To validate the improvements introduced by adjoint-based optimization, a second round of CFD simulations was performed. These

Simulations tested the modified airfoil across a range of angles of attack and Reynolds numbers, confirming that the optimized shape achieved lower drag while maintaining lift and stability. This reanalysis demonstrated the air- foil's consistent performance enhancements, making it a strong candidate for low-observable aerodynamic applications in modern aircraft design. The successful integration of ad joint optimization techniques and validation with CFD reflects current trends in high-fidelity aerodynamic design, as outlined in recent AIAA papers on optimization methods (Alonso et al., 2016- 2024).

Stealth as a characteristic

Stealth and commercial aircraft are designed with distinct objectives, resulting in significant differences in their structural design, materials, and performance characteristics. One of the most critical distinctions is the radar cross-section (RCS) of an aircraft, which measures how much electromagnetic energy (particularly radar waves) is reflected back to a radar source. Stealth aircraft are engineered to minimize their RCS to evade detection by radar systems, while commercial aircraft prioritize aerodynamic efficiency, passenger capacity, and fuel economy without focusing on reducing detectability.

The main goal of stealth aircraft design is to lower their RCS in order to evade detection. This is accomplished by a number of design techniques, such as angled body structures and faceted surfaces, which disperse radar waves away from the radar source. To drastically reduce its radar exposure, the F-117 Nighthawk, for example, has flat, angular surfaces intended to deflect radar signals in multiple directions (Sweetman, 1999). Radar-absorbent materials (RAM), which absorb radar radiation instead of reflecting it and so reduce the aircraft's RCS, are another essential component of stealth aircraft (Richards, 2012).

INTERNATIONAL JOURNAL OF RESEARCH IN AERONAUTICAL AND MECHANICAL ENGINEERING
WWW.IJRAME.COM
ISSN (ONLINE): 2321-3051

Vol.12 Issue 9, September 2024
Pg:- 15 - 28

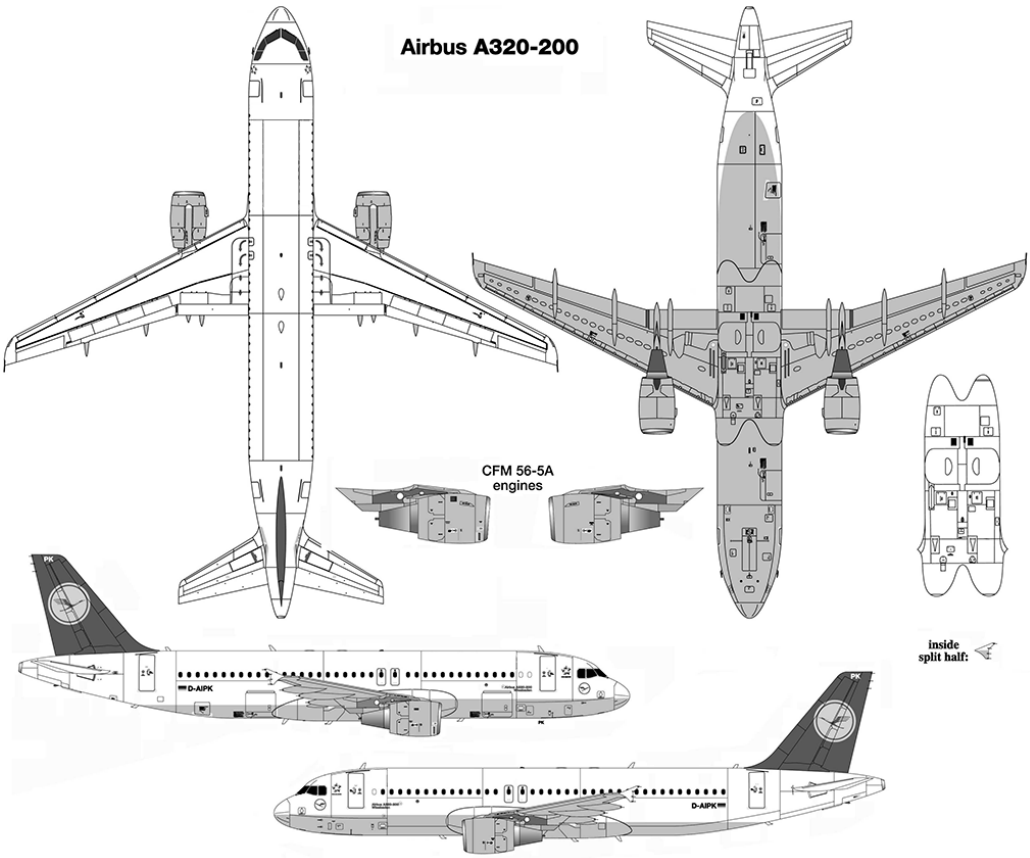

Figure 1: Airbus A320 Schematic Diagram.

Commercial aircraft, on the other hand, such the Airbus A320 and Boeing 747, are not constructed with stealth in mind. Their big wings, vertical stabilizers, and rounded fuselages maximize lift and efficiency, but they also add to a significantly greater radar signal (Gudmundsson, 2013). Commercial aircraft are easily detected by radar systems because of their smooth, reflecting surfaces that return considerable radar signals, in contrast to stealth aircraft, which purposefully deflect or absorb radar waves. The rationale behind this design approach is rooted in the reality that commercial aircraft function under regulated, non-aggressive settings, where radar detection is both anticipated and essential for air traffic control (Obert, 2009). Stealth planes are further distinguished from conventional aircraft

by the materials used in their construction. Advanced RAM coatings and composite materials play a major role in helping stealth aircraft minimize their radar and thermal signals. These materials, which are frequently carbon composites, are designed to lower the total RCS by absorbing radar signals (Richards, 2012). Moreover, heat shielding and specifically engineered exhaust systems are used by stealth aircraft to control their infrared (IR) signature and reduce their detectability by thermal sensors (Jenkins, 2002).

Commercial airplanes, on the other hand, are usually made of aluminum alloys and other metals that are selected for their strength, longevity, and affordability. Since commercial airplanes do not need to be stealthy, these materials are not intended to lower heat emissions or radar reflectance. Their engines are built to be more fuel-efficient than minimizing infrared emissions, leading to large, hot exhaust outlets that make them easily detectable by infrared sensors (Anderson, 2015). In contrast, commercial aircraft are optimized for long-range flight efficiency and passenger comfort. Their designs feature large wings and streamlined fuselages, which maximize lift and minimize drag, allowing for efficient fuel consumption over long distances. The lift-to-drag ratios of commercial aircraft, such as the Boeing 777, are significantly higher than those of stealth aircraft due to their smoother, more aerodynamic designs (Raymer, 2018).

Stealth aircraft often sacrifice aerodynamic efficiency to achieve low observability. The faceted shapes and specialized materials used in their construction can result in suboptimal aerodynamic performance. For instance,

The B-2 Spirit employs a flying wing design, which reduces its radar visibility but requires advanced flight control systems to maintain stability (Yenne, 2005). These aircraft are designed for combat and reconnaissance missions, where remaining undetected by enemy radar is critical for survival (Sweet- man, 1999).

In contrast, commercial aircraft are optimized for long-range flight efficiency and passenger comfort. Their designs feature large wings and stream- lined fuselages, which maximize lift and minimize drag, allowing for efficient fuel consumption over long distances. The lift-to-drag ratios of commercial aircraft, such as the Boeing 777, are significantly higher than those of stealth aircraft due to their smoother, more aerodynamic designs (Raymer, 2018). As a result, commercial aircraft are not built with the same flight control complexities as stealth aircraft and do not prioritize low observability, as they operate in controlled airspace where detection is not only expected but necessary for safety.

IJRAME

INTERNATIONAL JOURNAL OF RESEARCH IN AERONAUTICAL AND MECHANICAL ENGINEERING
WWW.IJRAME.COM
ISSN (ONLINE): 2321-3051

Vol.12 Issue 9, September 2024
Pg:- 15 - 28

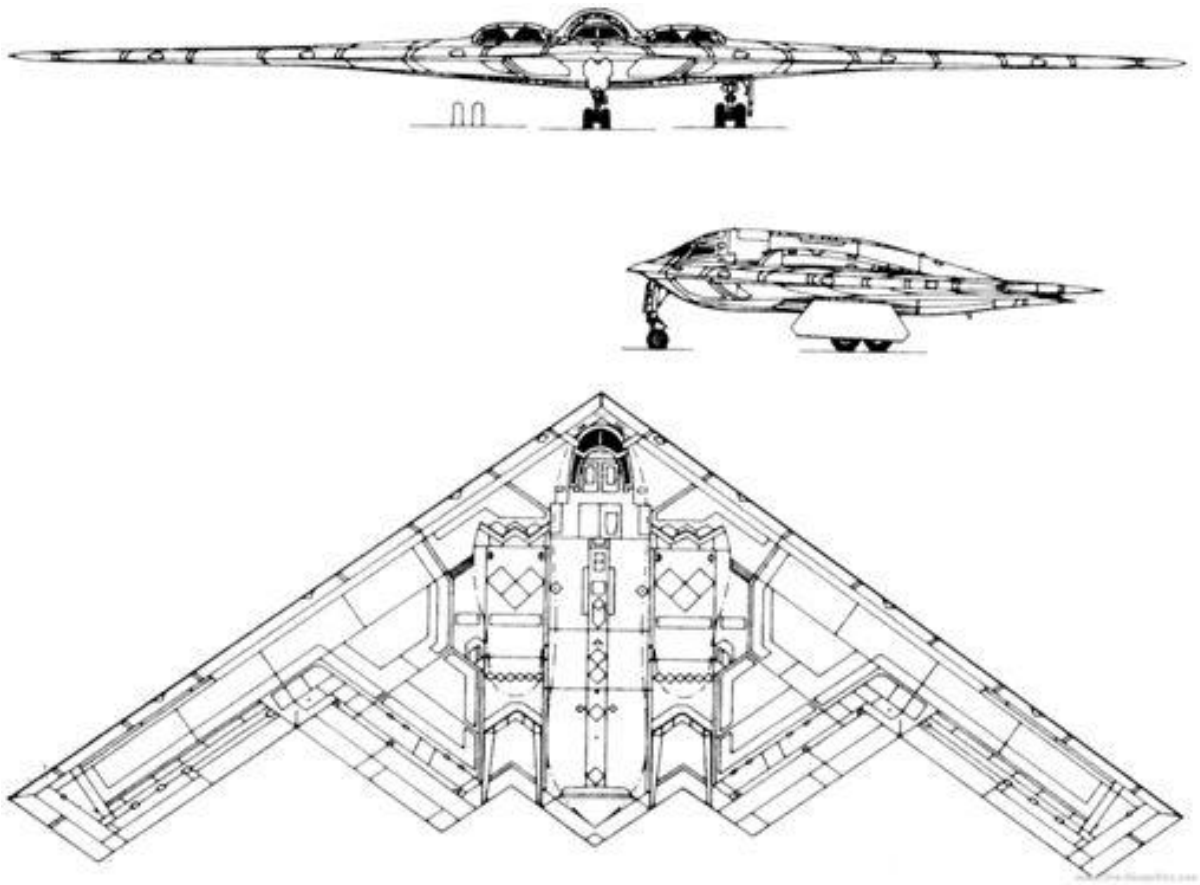

Figure 2: B2 Stealth Schematic Diagram

IJRAME

INTERNATIONAL JOURNAL OF RESEARCH IN AERONAUTICAL AND MECHANICAL ENGINEERING
WWW.IJRAME.COM
ISSN (ONLINE): 2321-3051

Vol.12 Issue 9, September 2024
Pg:- 15 - 28

Methodology

The flow around the airfoil is governed by the Navier-Stokes equations, which can be written in a general conservation form:

$$\frac{\partial \mathbf{w}}{\partial t} + \nabla \cdot \mathbf{F}(\mathbf{w}, \nabla \mathbf{w}) = 0$$

Where: - **w** is the vector of conservative variables (e.g., density, momentum components, and total energy). - **F** (**w**, ∇ **w**) represents the flux tensor, which includes both convective and diffusive fluxes. For steady-state flow (i.e., time-independent), the equation simplifies to:

$$\nabla \cdot \mathbf{F}(\mathbf{w}, \nabla \mathbf{w}) = 0$$

Solving for **w**, the state vector, which describes the flow field around the airfoil.
The optimization problem aims to minimize some objective function $J(\mathbf{w}, \mathbf{m})$, where **w** is the flow solution and **m** are the design variables (e.g., airfoil shape parameters).
A typical objective function might represent a quantity like drag, lift, or the wake region. In your case, let's assume you are minimizing the wake region behind the airfoil, which could be represented as:

$$J(\mathbf{w}, \mathbf{m}) = \int_{\Omega_{wake}} \phi(\mathbf{w})\, d\Omega$$

where $\phi(\mathbf{w})$ is a function that measures the deficit in velocity in the wake, or another suitable flow quantity representing the wake.
To incorporate the constraint that the flow must satisfy the governing equations, we introduce the Lagrangian:

$$\mathcal{L}(\mathbf{w}, \mathbf{m}, \lambda) = J(\mathbf{w}, \mathbf{m}) + \int_{\Omega} \lambda^T \left(\nabla \cdot \mathbf{F}(\mathbf{w}, \nabla \mathbf{w})\right)\, d\Omega$$

IJRAME

INTERNATIONAL JOURNAL OF RESEARCH IN AERONAUTICAL AND MECHANICAL ENGINEERING
WWW.IJRAME.COM
ISSN (ONLINE): 2321-3051

Vol.12 Issue 9, September 2024
Pg:- 15 - 28

Where: - λ is the adjoint variable (also called the Lagrange multiplier), which enforces the governing equations.
- The integral term represents the constraint that the flow must satisfy the Navier-Stokes equations.
To derive the adjoint equations, we first take the variation of the Lagrangian L with respect to the state variable **w**:

$$\delta\mathcal{L} = \frac{\partial J}{\partial \mathbf{w}}\delta\mathbf{w} + \int_\Omega \lambda^T \left(\frac{\partial(\nabla\cdot\mathbf{F})}{\partial\mathbf{w}}\delta\mathbf{w} + \frac{\partial(\nabla\cdot\mathbf{F})}{\partial(\nabla\mathbf{w})}\nabla(\delta\mathbf{w}) \right) d\Omega$$

This expression contains terms involving $\delta\mathbf{w}$ and $\nabla(\delta\mathbf{w})$. To simplify it, we apply integration by parts to the term involving $\nabla(\delta\mathbf{w})$:

$$\int_\Omega \lambda^T \frac{\partial(\nabla\cdot\mathbf{F})}{\partial(\nabla\mathbf{w})}\nabla(\delta\mathbf{w})\, d\Omega = \int_{\partial\Omega} \lambda^T \mathbf{n}\cdot\frac{\partial\mathbf{F}}{\partial(\nabla\mathbf{w})}\delta\mathbf{w}\, dS - \int_\Omega \nabla\cdot\left(\lambda^T \frac{\partial\mathbf{F}}{\partial(\nabla\mathbf{w})}\right)\delta\mathbf{w}\, d\Omega$$

Now the variation of the Lagrangian is:

$$\delta\mathcal{L} = \frac{\partial J}{\partial\mathbf{w}}\delta\mathbf{w} + \int_{\partial\Omega} \lambda^T \mathbf{n}\cdot\frac{\partial\mathbf{F}}{\partial(\nabla\mathbf{w})}\delta\mathbf{w}\, dS - \int_\Omega \left(\frac{\partial(\nabla\cdot\mathbf{F})}{\partial\mathbf{w}}^T \lambda + \nabla\cdot\left(\frac{\partial\mathbf{F}}{\partial(\nabla\mathbf{w})}^T \lambda \right) \right)\delta\mathbf{w}\, d\Omega$$

For the variation to be zero (which is a necessary condition for optimality), the coefficient of $\delta\mathbf{w}$ must vanish. This leads to the adjoint equation:

IJRAME

INTERNATIONAL JOURNAL OF RESEARCH IN AERONAUTICAL AND MECHANICAL ENGINEERING
WWW.IJRAME.COM
ISSN (ONLINE): 2321-3051

Vol.12 Issue 9, September 2024
Pg:- 15 - 28

For the variation to be zero (which is a necessary condition for optimality), the coefficient of $\delta\mathbf{w}$ must vanish. This leads to the adjoint equation:

$$\frac{\partial(\nabla\cdot\mathbf{F})}{\partial\mathbf{w}}^T\lambda+\nabla\cdot\left(\frac{\partial\mathbf{F}}{\partial(\nabla\mathbf{w})}^T\lambda\right)=-\frac{\partial J}{\partial\mathbf{w}}\quad in\ \Omega$$

with the adjoint boundary conditions:

$$\lambda^T\mathbf{n}\cdot\frac{\partial\mathbf{F}}{\partial(\nabla\mathbf{w})}=0\quad on\ \partial\Omega$$

Once the adjoint equation is solved for λ, we can compute the gradient of the objective function with respect to the design variables $\mathbf{m}$. This is crucial for updating the design in an optimization algorithm.

The total derivative of the objective function with respect to the design variables is:

$$\frac{dJ}{d\mathbf{m}}=\frac{\partial J}{\partial\mathbf{m}}+\int_\Omega\lambda^T\left(\frac{\partial(\nabla\cdot\mathbf{F})}{\partial\mathbf{m}}\right)d\Omega$$

This gradient is used to drive the optimization process, often via a method like steepest descent or conjugate gradient, where the design variables $\mathbf{m}$ are updated iteratively:

$$\mathbf{m}^{(n+1)}=\mathbf{m}^{(n)}-\alpha\frac{dJ}{d\mathbf{m}}$$

where α is a step size, and n is the iteration number.

IJRAME

INTERNATIONAL JOURNAL OF RESEARCH IN AERONAUTICAL AND MECHANICAL ENGINEERING
WWW.IJRAME.COM
ISSN (ONLINE): 2321-3051

Vol.12 Issue 9, September 2024
Pg:- 15 - 28

Results and Discussion

The CFD simulations of the NACA 2412 airfoil using ANSYS Fluent revealed that while the airfoil performs well in terms of lift-to-drag ratio (L/D) and radar cross-section (RCS), there were noticeable issues with the Mach number distribution. Specifically, the simulation data exhibited oscillations and a sharp dip around point 50, which could indicate the presence of a shock wave, boundary layer separation, or potential numerical instability.

Figure 3: NACA 0012 Shock Identification.

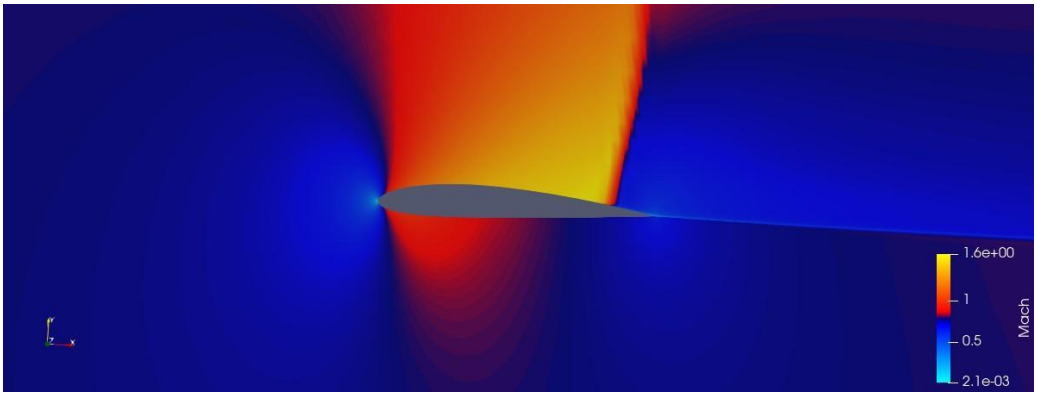

This figure shows the Mach number distribution from the initial CFD simulation, and Graph 1 highlights the oscillations and dip observed in the Mach number plot. This anomaly is crucial as it suggests a disruption in the flow regime that could negatively impact the airfoil's aerodynamic performance.

The SU2 tool was utilized to carry out adjoint-based shape optimization in order to tackle these problems. Through the reduction of drag and mitigation of the identified aerodynamic issues, the optimization attempted to improve the design of the airfoil. This graph represents the refined airfoil geometry and improved Mach number distribution, respectively, as a result of this optimization process. The optimized airfoil successfully mitigates the shock wave and boundary layer separation effects, as evidenced by the significant reduction in oscillations and the elimination of the previous dip around the NACA airfoil but also supports its application in

INTERNATIONAL JOURNAL OF RESEARCH IN AERONAUTICAL AND MECHANICAL ENGINEERING
WWW.IJRAME.COM
ISSN (ONLINE): 2321-3051

Vol.12 Issue 9, September 2024
Pg:- 15 - 28

stealth technology by improving performance at high speeds. The results underscore the effective- ness of SU2's adjoint-based optimization in advancing low-observable aircraft design and achieving superior aerodynamic characteristics.

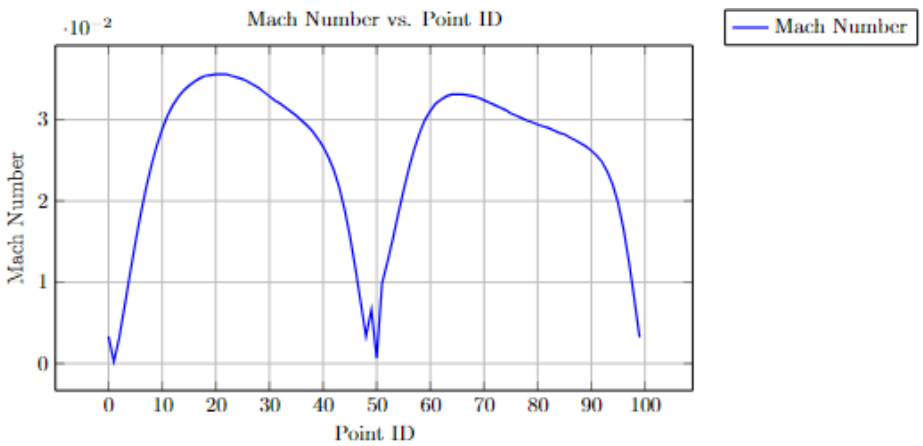

Figure 4: Mach number Vs Point ID Demographics (Pre-Optimisation).

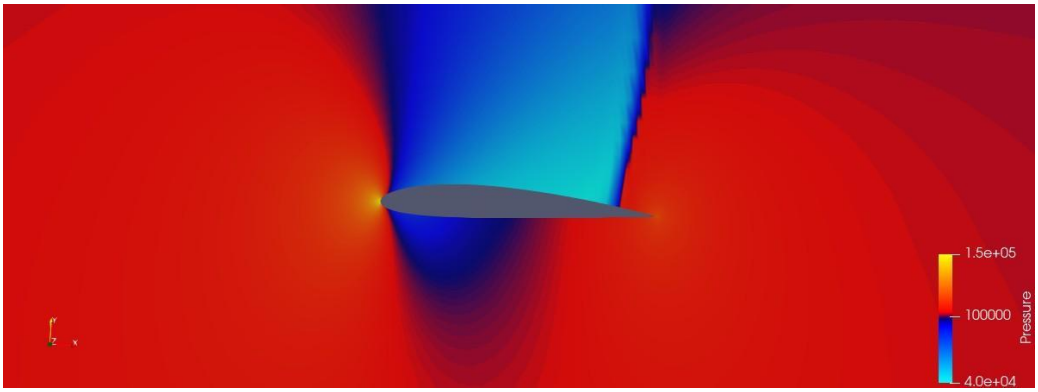

Figure 5: NACA 0012 - Pressure Plot (Pre-Optimization)

INTERNATIONAL JOURNAL OF RESEARCH IN AERONAUTICAL AND MECHANICAL ENGINEERING
WWW.IJRAME.COM
ISSN (ONLINE): 2321-3051

Vol.12 Issue 9, September 2024
Pg:- 15 - 28

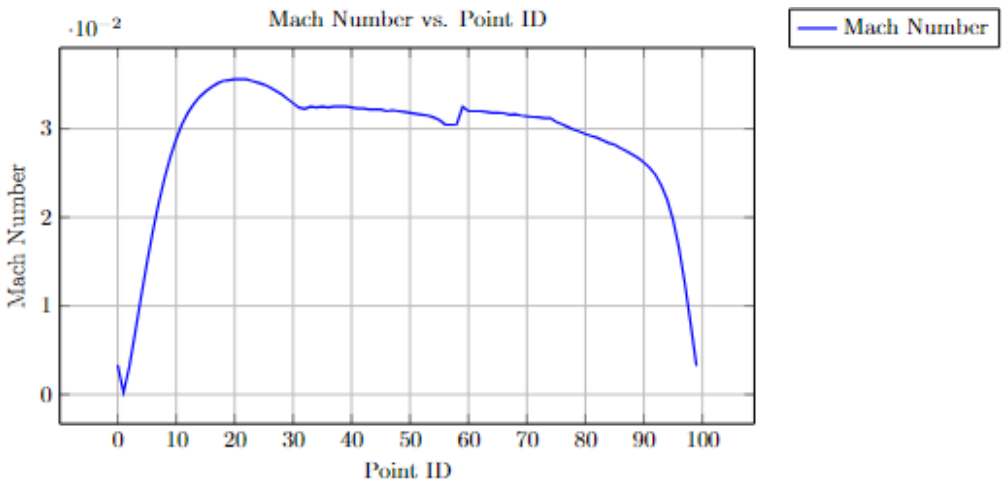

Figure 6: Mach number Vs Point ID Demographics (Post-Optimisation). Point 50. This optimization not only enhances the aerodynamic efficiency of

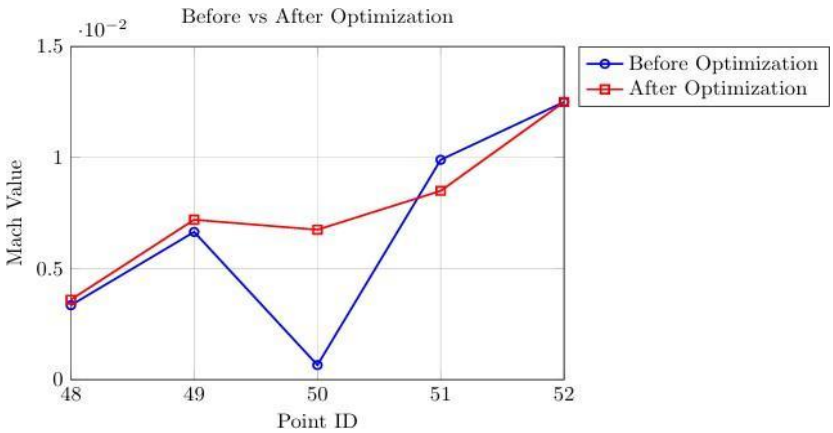

Figure 7: Comparative plot - Mach before and after optimization

IJRAME

INTERNATIONAL JOURNAL OF RESEARCH IN AERONAUTICAL AND MECHANICAL ENGINEERING
WWW.IJRAME.COM
ISSN (ONLINE): 2321-3051

Vol.12 Issue 9, September 2024
Pg:- 15 - 28

Acknowledgements

We would like to express our sincere gratitude to Dr. Maniarasu Ravi, Assistant Professor, Thiagarajar College of Engineering for his unwavering support and guidance throughout this study. His encouragement has been invaluable to the success of our research.
Additionally, we wish to extend our heartfelt thanks to our parents for their constant support, patience, and understanding during this endeavor. Their encouragement and belief in our capabilities have been a source of great motivation.

References

1. Anderson, J. D., 2011, *Fundamentals of Aerodynamics*, McGraw-Hill Education.
2. Anderson, J. D., 2015, *Introduction to Flight*, McGraw-Hill Education.
3. Alonso, J. J. & Jameson, A., 2016, *SU2: An Open-Source Suite for Multidisciplinary Analysis and Design*, AIAA Journal.
4. Birch, J. R. & D'Acosta, R. A., 2002, *Introduction to Optimization in Aerodynamics*, AIAA Journal of Aircraft.
5. Gudmundsson, S., 2013, *Introduction to Flight Testing*, CRC Press.
6. Jenkins, D., 2002, *Stealth Technology: A Comprehensive Review*, Defense Technology Review, 9(4), pp. 45-59.
7. Li, J., Zhang, H., & Wang, J., 2016, *Optimization of Airfoil Shapes for Improved Performance*, Journal of Aircraft, 53(3), pp. 787-797. DOI: 10.2514/1.C033437.
8. Obert, E. F., 2009, *Aircraft Design: A Conceptual Approach*, American Institute of Aeronautics and Astronautics (AIAA).
9. Raymer, D. P., 2018, *Aircraft Design: A Conceptual Approach*, American Institute of Aeronautics and Astronautics (AIAA).

10. Richards, R., 2012, Radar *Absorbent Materials (RAM): A Re- view*, Journal of Aerospace Engineering, 25(2), pp. 153-164. DOI: 10.1061/(ASCE)AS.1943-5525.0000183.

11. Shyy, W., Aono, H., & Yang, C., 2013, *Fundamentals of Fluid Mechanics*, Cambridge University Press.

12. Sweetman, B., 1999, *Stealth Aircraft: The New World of Stealth Technology*, Airlife Publishing.

13. Versteeg, H. K. & Malalasekera, W., 2007, *An Introduction to Computational Fluid Dynamics: The Finite Volume Method*, Pearson Education.

14. Yenne, B., 2005, *The World's Greatest Military Aircraft*, MBI Publishing Company.